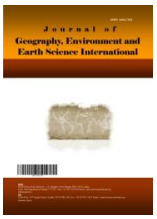

Journal of Geography, Environment and Earth Science International

23(4): 1-20, 2019; Article no.JGEESI.53078
ISSN: 2454-7352

Analysis of the SWAT (Soil and Water Assessment Tool) Semi-distributed Model Input Data for the Hydrological Simulation of the Lobo Water Reservoir (Central West of Côte d'Ivoire)

T. J. J. Koua[1*], K. H. Kouassi[1] and K. A. Anoh[1]

[1]UFR Environment, Laboratory of Environmental Sciences and Technologies, Jean Lorougnon Guedé University, BP 150 Daloa, Côte d'Ivoire.

Authors' contributions

This work was carried out in collaboration among all authors. Author TJJK designed the study, performed the statistical analysis, wrote the protocol and wrote the first draft of the manuscript. Authors TJJK and KHK managed the analyses of the study. Author KAA managed the literature searches. All authors read and approved the final manuscript.

Article Information

DOI: 10.9734/JGEESI/2019/v23i430182
Editor(s):
(1) Dr. Suvendu Roy, Assistant Professor, Department of Geography, Kalipada Ghosh Tarai Mahavidyalaya, India.
Reviewers:
(1) R. K. Mathukia, Junagadh Agricultural University, India.
(2) Jayath P. Kirthisinghe, University of Peradeniya, Sri Lanka.
(3) Rose Edwin Daffi, University of Jos, Nigeria.
Complete Peer review History: http://www.sdiarticle4.com/review-history/53078

Original Research Article

Received 06 October 2019
Accepted 12 December 2019
Published 23 December 2019

ABSTRACT

This study aims to analyze the input data of the semi-distributed SWAT model that can be used as a hydrological study of the Lobo water reservoir. The adopted approach includes two major steps: The input data estimation and the watershed configuration. The estimation of input data consists in the collection and calculation of input data necessary for the watershed configuration. The input data collected and estimated were a digital elevation model (DEM), a soil map, soil physico-chemical parameters (grain size, K erodibility coefficient, exchangeable anions, soil density, organic carbon, soil electrical conductivity), a land cover map, information on agricultural practices and daily climate data (Temperature, Rainfall, Sunshine, Wind Speed and Relative Humidity). The watershed configuration consisted of the extraction of watershed boundaries and watershed network, the integration of data, the calculation of hydrological response units (HRU) and the watershed

**Corresponding author: E-mail: kouatanoh7@gmail.com;*

configuration. The SWAT model permitted to extract a single type of soil for Lobo water reservoir watershed. The watershed has a dense drainage system which means that the area is heavily drained. The degraded forest occupies 37% of the watershed followed by agricultural land (30% of the territory). 213 HRU from 39 sub-watersheds were also obtained. These data are an indispensable tool for the hydrological simulation of the Lobo reservoir.

Keywords: SWAT; Lobo River; agro-hydrological modeling; Daloa; water reservoir; HRU.

1. INTRODUCTION

The need to assess the impact of global changes in agrosystems and ecosystems, and the consequences of major disturbances such as floods, droughts and water resources pollution, creates new requirements for hydrological modeling. The success of this modeling depends on the ability to understand the hydrological processes in the different compartments of the water cycle and to manage spatial information in relation to these processes [1]. The first step in any scientific process is to observe and identify a set of variables that can describe the phenomenon or process being studied [2]. This knowledge remains encyclopedic and of little interest as long as no link or relationship is established between a first set of variables (input variables such as hydroclimatic data) and another set of variables subject to the first set of variables (output variables such as flow rates, evapotranspiration). These variables are a function of time and space. The characterization of the time and space variables that govern the hydrological cycle, as well as the analysis of changes in surface conditions, are essential for the effective management of water in a watershed [3]. The diversity of the processes involved (physical, chemical and biological processes), the complexity of the systems studied (multiple boundary conditions and the difficulty of considering a "closed" system), the presence of multiple scales, both spatial and temporal, the difficulty of extensive measurements and under a variety of conditions have led to the development of new technologies (SWAT, ArcGIS, ENVI). New technologies and digital tools are presented as tools adapted to the knowledge of water resources [4] as well as for their rational management [5]. In recent decades, the development of mathematical models has made water resources management more flexible through the implementation of hydrological models. This allows not only to evaluate water resources, but also to plan, develop and propose solutions to problems of civil engineering, quantitative and qualitative water management, soil conservation, etc. Several types of models can describe these hydrological processes. Among these models, we can cite the physical-based conceptual models: A model in which the functioning of the basin is presented by an analogy, a concept. The analogy most often used to represent the functioning of soils and groundwater is that of the tank whose discharge rate depends on the filling rate. These are models based on known physical processes [6,7]. The whole operation is a compromise between a precise physical representation of certain phenomena and a more empirical representation for others. There exists between measurable quantities in reality and those measurable on the model of similarity ratios which can be calculated a priori and which ensure the full-scale transferability of the results obtained on the model. The justification of the model ultimately rests on the fact that the same equations govern the phenomena in full scale and reduced model. There are also empirical models that are developed from laboratory or field experiments [8]. This is the case, for example, of the USLE (Universal Soil Loss Equation) erosion model [9]. These two types of models can then be global such as the GR4 model, that is to say that they apprehend the watershed as a single entity, and tries to reproduce its general behavior. Unfortunately, the global model does not take into account the spatial variability of the parameters governing phenomena such as runoff or erosion and therefore cannot assess the effects of changes in land use or use and territory in general. This is why so-called distributed models, such as the Soil and Water Assessment Tool (SWAT), have been developed, making it possible, using more complex mathematical formulas, to represent the spatial variability of the phenomena acting on the basin. This is thus divided into units in order to take into account the heterogeneity of the characteristics influencing its hydrological response. With these, it becomes possible to make an increasingly fine representation of a hydrosystem, seat of various hydrological processes with multiple and complex interactions, integrating natural parameters and/or related to human activities [10]. Taking

into account the probable changes to the territory, it is possible to describe the observations of the territory or watershed from the variables of the model. However, these models are very complex and require a very large number of parameters. Their applicability is thus reduced because very few basins have very detailed and continuous databases. The watershed of the Lobo water reservoir, like most West African basins, does not have sufficient data for a rigorous hydrological study, hence the need for this study using of the SWAT model. The SWAT model was validated in the United States in the Chesapeake Bay watershed by Wagena et al. [11] for the study of agricultural conservation practices that can help mitigate the impact of climate change. It has also been successfully used in China by Bai et al. [12] to evaluate the effectiveness of vegetative filter strips in reducing faecal coliforms based on a modified soil and water assessment tool.

In Côte d'Ivoire, SWAT has been used successfully to simulate flows and assess the impacts of climate change in the Buyo Lake watershed [13,14,15].

The objective of this study is to analyze the input data of the SWAT model that can be used to study the hydrological behavior of the Lobo water reservoir.

2. MATERIALS AND METHODS

2.1 Study Area

The water reservoir of Lobo is located on the Lobo River a tributary of the Sassandra River. Its watershed is located in west-central Côte d'Ivoire between 6°21 and 6°35 West Longitude and 6°54 and 7°01 North Latitude (Fig. 1). The Lobo reservoir has its source in the region of Séguéla, drains an area of 12,745 km ² and travels 355 km with a perimeter of 530 Km. The relief of the basin, little contrasted and little varied is dominated by trays of 200 m to 400 m altitude [16]. The geological formations that cover this watershed are mainly composed of granites, to which are added some intrusions of shale and flysch. The watershed of Lobo is located in the Guinean domain. It belongs to the great tropical humid region. It is characterized by two rainfall maxima obtained in September (275 mm) and May (150 mm). The two rainy seasons are separated by the long dry season from November to February. In the Buyo region, there are two major seasons. Eight months of rainy season and four months of season at two maximum rainfall. The month of June represents the peak of the great rainy season and that of September the peak of the short rainy season. The two maxima are separated by one or two months more or less rainy. The annual water balance shows 1518.5 mm of rain, runoff of 236 mm, infiltration of 456 mm and actual evapotranspiration of 805 mm. The vegetation is composed of dense moist semi-deciduous forest with cleared mesophilic forest. The soils encountered are ferralitic type strongly or moderately desaturated. Economic activities are quite diversified, but agriculture remains the main income generating activity. It occupies the majority of the populations. Agricultural dynamics is based essentially on perennial cash crops (coffee, cocoa, rubber, oil palm), food crops and market gardeners. The agricultural system initially extensive, today evolves towards a much more intensive agriculture because of the scarcity of arable land [17]. The drinking water supply of the populations is ensured by the water supply systems of SODECI for the big urban centers and by the system of village hydraulics (HV) and improved village hydraulics (HVA) for the others localities.

2.2 Material

2.2.1 Data

2.2.1.1 Digital Elevation Model (DEM)

The Digital Elevation Model (DEM) (Fig. 2) describes the elevation of any point in the study area at a specific spatial resolution. It was used to delineate the watershed and extract the hydrographic network. The DEM used has a resolution of 30 m x 30 m and is downloaded from the website https://search.earthdata.nasa.gov/search.

2.2.1.2 Satellite images of sentinel mission 2

An image of sentinel-2 satellite images of February 22, 2018, with a resolution of 10 m, were used for mapping the land use. This image includes four (4) bands that are 2, 3, 4 and 8. these images have been uploaded to the website https://scihub.copernicus.eu/dhus/#/home.

2.2.1.3 Soil data

The swat model requires different textural and physicochemical properties of the soil such as texture, available water content, hydraulic conductivity, bulk density and organic carbon content of different soil layers. These data come

from the FAO soil database [18]; they were supplemented by physico-chemical data acquired after sampling in the field and in the laboratory.

2.2.1.4 Climate data

The meteorological data used have a daily time step. These are minimum and maximum temperatures, precipitation, relative humidity, solar radiation and wind speed. These data were obtained from the swat model website http://globalweather.tamu.edu/. They cover the period 1979-2014. The four climatic stations are used (Fig. 3).

2.2.2 Computer software

This study was conducted with three main softwares. The Arcswat software in the ArcGIS 10 interface was used to delineate the watershed and sub watersheds, and to extract the river system. ArcGIS 10 allowed the digitization of certain data and geo-processing. The envi 4.7 software allowed the digital processing of satellite images to obtain the land use map; and the WGN parameters Estimation Tool software was used to calculate the statistical parameters of the climate data.

2.3 Methods

The methodology adopted to achieve the objective includes: the processing of the Digital Elevation Model (DEM), the satellite images processing, the calculation of the hydro-statistical parameters, the integration of the land use and soil maps and the calculation of hydrological response units (HRU).

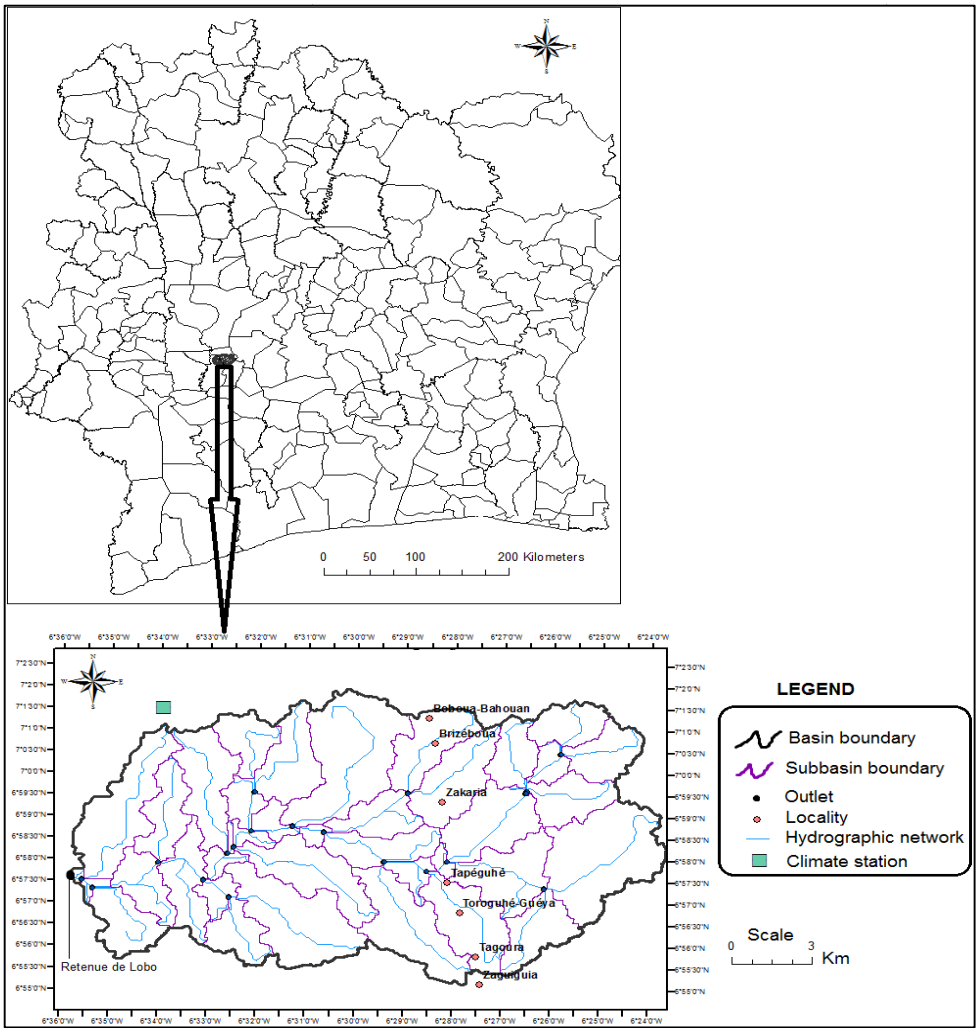

Fig. 1. Overview of the lobo watershed contribution

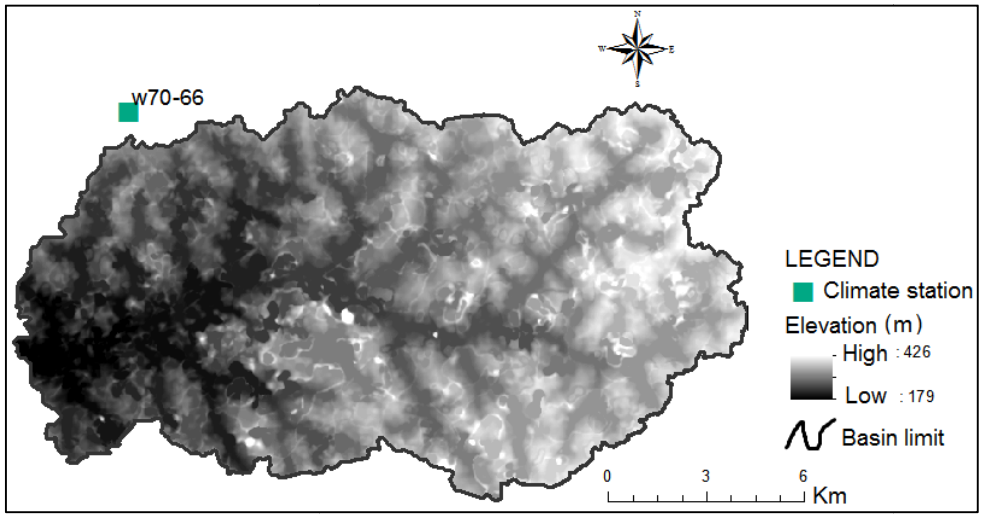

Fig. 2. Digital elevation model (DEM) of the lobo reservoir sub basin contribution

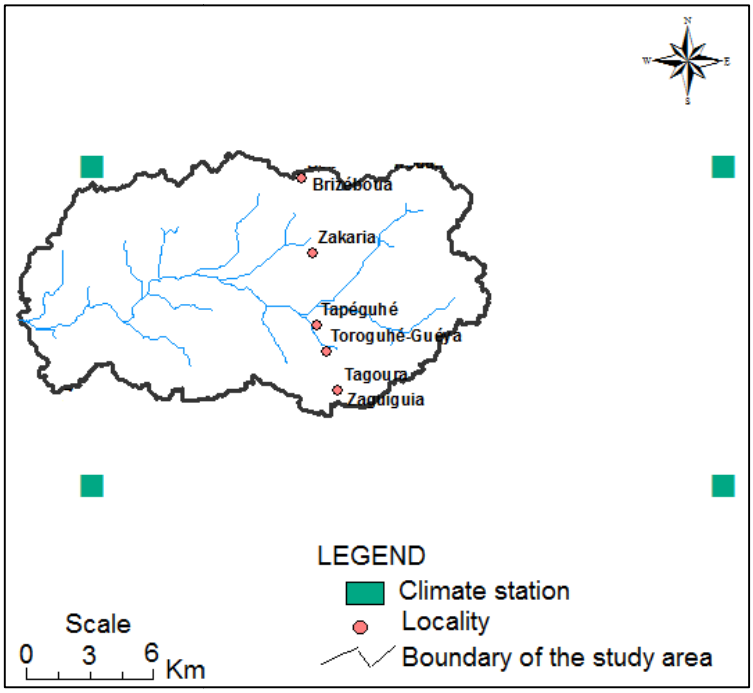

Fig. 3. Climate stations in the study area

2.3.1 Processing of the Digital Elevation Model (DEM)

From the DEM, the watershed boundaries and its hydrographic network are extracted. Thanks to the coupling of the ArcGis software with the Swat model, the extraction of the limits is almost automatic and uses a classical method implementing the treatments of the algorithm (D8) of Jenson and Domingue [19]. The algorithm used is called D8 (Fig. 4), because it considers the flow directions following unidirectional flow in eight connections, taking into account the eight neighboring cells of the considered point [20]. This treatment is carried out by the following steps: filling of the low points and calculation of the slopes (flow accumulation), the flow directions determination (flow direction), calculation of the drained surfaces and extraction of the hydrographic network.

2.3.2 Satellite image processing

Land use can be briefly defined as the physical (and biological) cover of the land surface [21]. Different natural and anthropogenic processes intervene and modify the state of the land use. The flows are thus influenced by the surface states. Surface conditions were used to estimate flows in several basins [22]. Therefore, it seems essential in any study of hydrological behavior of a watershed to know the land cover. For the knowledge of land-use classes in the Lobo watershed, we used a Sentionel-2 image that described the natural landscape of the basin. These are images from February 22, 2018. The availability, the spatial resolution and the sharpness of the image (absence of cloud coverings) guided this choice. Seven land cover classes were identified: dense forest, degraded forest, grass cover, agriculture, medium density habitat, water and wetland. The methodology for mapping land use is presented in Fig. 5.

The supervised classification is performed using the Maximum Likelihood algorithm based on Google Earth imagery and field data. The maximum likelihood method is a parametric estimation method. It is based on the following idea: having observed the values x1,. . . , xn is not surprising, "or again: the hypothesis of observing the values x1, ..., xn rather than others was the most likely".

Thus, the likelihood of the data x1,. . . , xn can be defined by the function of θ:

$$L_n(\theta) = \mathbb{P}_\theta\left(\bigcap_{i=1}^{n}\{X_i = x_i\}\right) = \prod_{i=1}^{n}\mathbb{P}_\theta(X_i = x_i) = \prod_{i=1}^{n}\mathbb{P}_\theta(X = x_i) \quad (1)$$

The identity and location of specific sites representing homogeneous regions in the image were obtained through the combination of field observations and map data. these regions are commonly referred to as training sites because the spectral characteristics of these regions are used to drive the classifier that is here, the maximum likelihood algorithm that we used to classify the rest of the image.

2.3.3 Calculation of hydro statistics parameters

The hydro statistical parameters of the climate data were calculated using SWAT's WGN parameters Estimation tool [23]. The parameters calculated from daily data are: the average daily maximum temperature in the month (TMPMX), the minimum daily average temperature in the month (TMPMN), the standard deviation of the maximum daily temperature in the month (TMPSTDMX) , the standard deviation of the daily minimum temperature in the month (TMPSTDMN), the mean total monthly precipitation (PCPMM), the standard deviation of the mean total monthly precipitation (PCPSTD), the asymmetry coefficient of the daily precipitation in the month (PCPSKW), the probability that a wet day follows a dry day in the month (PR_W1, mon), the probability that a wet day follows a wet day in the month (PR_W2, mon), the average number of rainy days in the month (PCPD), the maximum precipitation of half an hour of rain in the month (RAINHHMX), the average daily insolation in the month (SOLARAV), the relative humidity (HMD) expressed in fractional form, the average daily wind speed in the month (WNDAV).

2.3.4 Integration of the land use map and the soil map

The land use and soil maps were integrated into the swat model using the tool '' land use / soils / slope definition ''. it was necessary first to make a correspondence of the land use and pedological classes with those recognized by the SWAT model. A reclassification was subsequently necessary to represent the different classes according to the specific types in connection with the SWAT database.

2.3.5 HRU calculation and basin configuration

The hydrological response unit (HRU) is the basis for calculation in SWAT model. It is the combination of a single type of land use, soil and slope. HRUs allow the model to reflect differences in evapotranspiration and other hydrologic conditions for different soil cover. Runoff is estimated separately for each HRU and routed to achieve total runoff for the watershed. The land use classes were defined using the "look up table" table. This table, which identifies the 4 SWAT code letters for the different soil cover / land use categories, was prepared to match soil / land cover values with those predefined in SWAT followed by reclassification. Like land use, the soil layer has been reclassified. Slope classes have also been incorporated into the definition of hydrological response units. Then, the land use map, the soil map and the slope were superimposed to determine the HRU. The last step was HRU definition. The distribution of the HRU in this study was determined by assigning the "multiple

HRU" option to each sub watershed. In the "multiple definition" mode, a threshold was used to eliminate minor values of land use, pedology and slope classes in each sub-basin and the remaining slopes were redistributed so that the entire basin to model is covered.

Once the HRUs are calculated, SWAT will proceed to write the different tables of input data. These data tables are related to general watershed configuration, soil data, hydro-meteorological data, general sub watershed data, HRUs, main watershed channels, groundwater, and water use, water, watershed management, soil chemistry, wetlands, river water quality, septic tanks, watershed practices, general watershed water quality of the watershed and the master file of the watershed. These data relating to the different compartments of the watershed can be updated at any time according to the need.

At this stage, the hydrological behavior of the catchment basin of the lobo water reservoir can be simulated.

The methodology adopted can be summarized from Fig. 6.

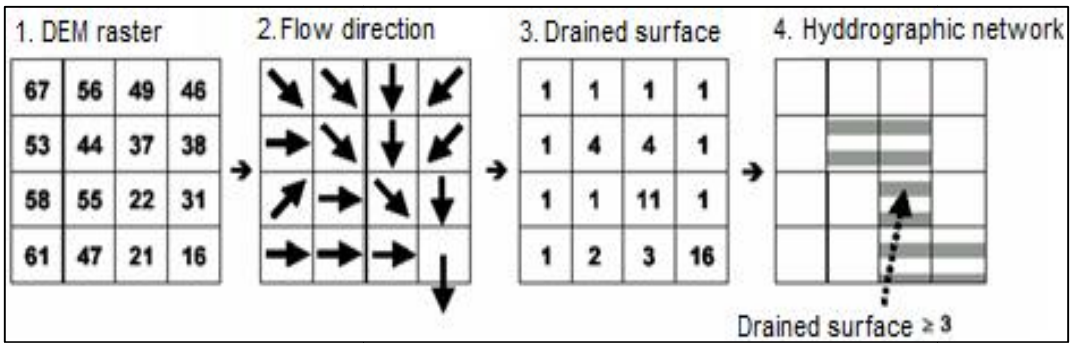

Fig. 4. Calculation of the hydrographic network by the D8 method with a threshold of drained upstream surface [20]

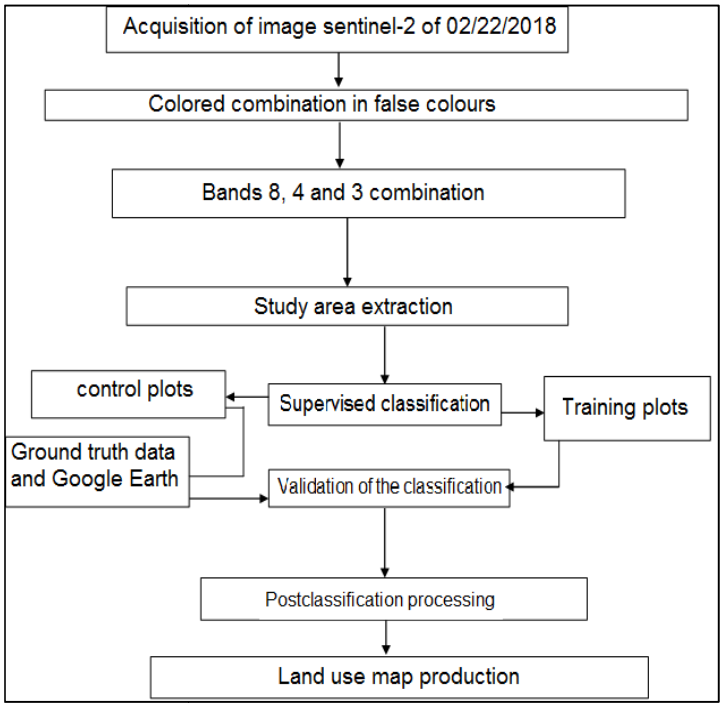

Fig. 5. Land use map methodology for the Lobo Reservoir sub basin contribution

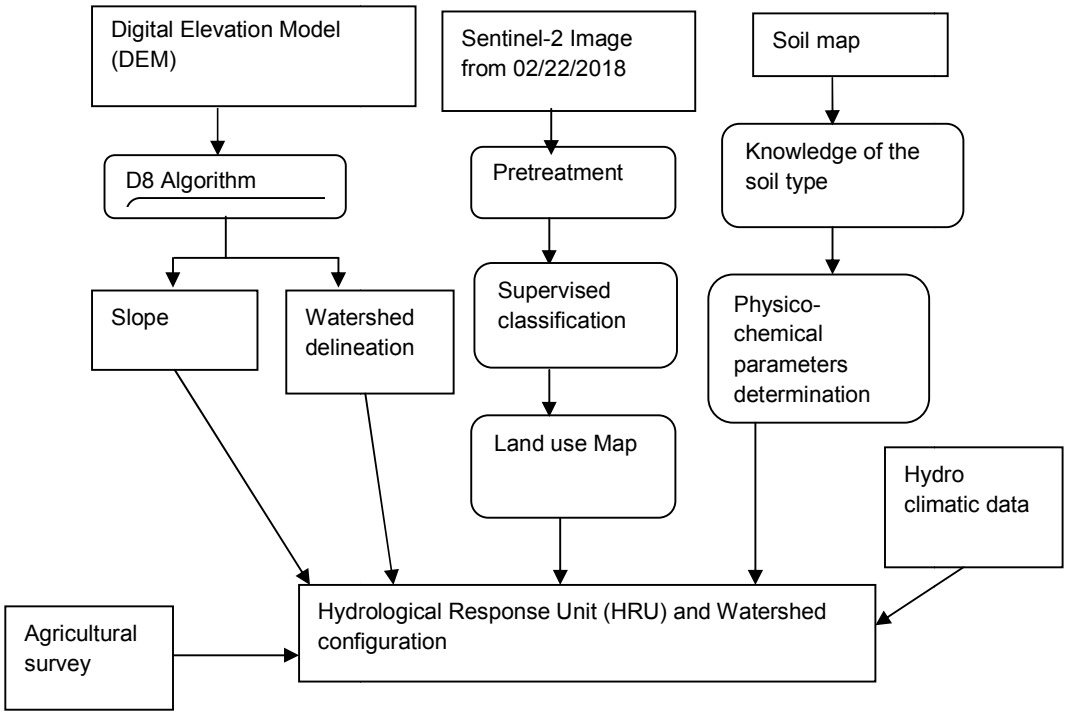

Fig. 6. HRU calculation and watershed configuration methodology

3. RESULTS AND DISCUSSION

3.1 Results

3.1.1 Watershed characteristics

The delineation of the watershed and the extraction of the hydrographic network had led obtaining 39 sub watersheds according to the configuration of the zone relief and the hydrographic network (Fig. 7). The watershed has an area of 205.83 km^2 and a perimeter of 101.32 km, giving a Gravelius (KG) compaction index of 1.98. The watershed is therefore elongated. The minimum altitude is 200 m (outlet) while the maximum altitude is 399 m. The watershed has a dense hydrographic network that allows feeding of the Lobo water reservoir in any season.

3.1.2 Land cover in the watershed

From the Sentinel-2 image processing, the land use (cover) map obtained is shown in Fig. 8. This map shows seven land use classes that are: agriculture, dense forest, degraded forest, grassy vegetation, medium density habitat, water and wetlands. The classification gave a confusion matrix with an overall accuracy of 83% and a Kappa of 80% (Table 1). These values indicate overall satisfaction with the classification. Agriculture occupies 30%, dense forest 4%, degraded forest 37%, medium density habitat 3%, grassland 22%, water 0.3% and wetlands 3%. The degraded forest occupies 37% of the watershed followed by agricultural land occupying 30% of the territory.

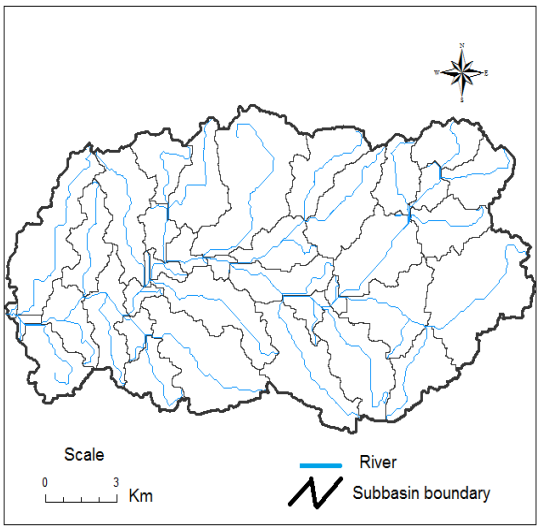

Fig. 7. Hydrographic network of the Lobo watershed contribution

3.1.3 Hydro statistic parameters

3.1.3.1 Maximum daily temperatures

The maximum daily average monthly temperature (TMPMX) calculated over the period 1979-2014 oscillates between 27 and 37ºC. The maximum temperature is observed in February, the lowest being recorded in August (Tables 2 and 3). The standard maximum temperature deviations (TMPSTDMX) change from 1.9 to 3.5 ^{o}C. The differences between maximum temperatures are very pronounced in the months of March, April and May (Tables 4, 5 and 6). These deviations show a significant variation in maximum temperatures during the month.

3.1.3.2 Minimum daily temperature

The results indicate monthly mean daily minimum temperatures (TMPMN) ranging from 18 to 23ºC (Tables 3 and 4). The lower temperature is observed in January in full Harmattan; the higher temperature is found in April at the beginning of the rainy season. The standard minimum temperature standard deviations (TMPSTDMN) change from 0.7 to 3.5ºC. The largest differences occur in January and December in the dry season with values up to 3.5 (Tables 6 and 7). These deviations show a significant variation in maximum temperatures during the month.

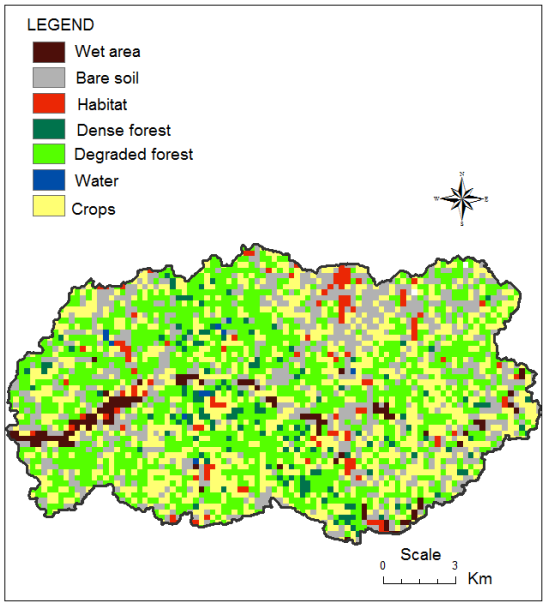

Fig. 8. Land cover map of the Lobo Reservoir watershed contribution

3.1.3.3 Daily rainfall

Average daily precipitation in the month (PCPMM) is between 17 and 262 mm (Tables 7 and 8). The standard deviations vary from 1.8 to 12.52 mm over the entire watershed (Tables 8 and 9). Compared to temperatures, the differences in rainfall are greater. The precipitation asymmetry coefficient (PCPSKW) changes from 2.14 to 20.46. The higher asymmetry coefficients values are observed in December while the lowest values are in November (Tables 9 and 10). All asymmetric coefficients are greater than 0. This indicates that the rainfall distribution is asymmetrical to the left on the watershed. The computation of the probability that a wet day follows a dry day (PR_W1, mon) shows values ranging between 0 and 1. The month of September presents weak probabilities around 0, the higher probabilities (1) is observed in October (Tables 11 and 12). The probability that a wet day follows another wet day (PR_W2, mon) evolves from 0.78 to 1. In January, the low values are generally noted whereas the highest ones are observed in August, September and October (Tables 11 and 13). Based on the number of rainy days in the month (PCPD), it appears that it rains more in the months of July, August, September and October (Tables 13 and 14). The maximum precipitation of half an hour of rain in the month (RAINHHMX) ranges from 2.07 to 15.22 mm (Tables 14 and 15). In the month of January, there is a maximum rainfall of half an hour of rain. In May, this parameter increases and reaches 15.22 mm of rain.

3.1.3.4 Average daily solar radiation in the month (SOLARAY)

Solar radiation values are between 13.3 and 20.47 MJ/m^2/day (Tables 15 and 16). These results show that sunshine remains important in the dry season (January, February, March) where values of up to 20.47 MJ/m^2/day are obtained. These values begin to fall from April until August with the onset of the rainy season. From September, a recovery is initiated. This recovery continues until December to reach values of 18.92 MJ/m^2/day.

3.1.3.5 Relative Humidity (HMD)

The relative humidity in fractional form varies from 0.54 to 0.89. The low relative humidity values are observed in January and February with values between 0.54 and 0.65. The period

May-November remains very wet with values between 0.8 and 0.89 (Tables 17 and 18).

3.1.3.6 Average daily wind speed in the month (WNDAV)

Wind speed varies from 1.2 to 1.82 m/s over the entire watershed (Table 18). Stronger winds are observed in the months of March, April, July and August where we can record wind blowing at more than 1.8 m/s.

3.1.4 Map of land use and pedological discretized by sub-watershed

The water budget is calculated by sub-watershed, the land use and pedology are discretized by sub-watershed in order to know the influence of these parameters on the hydrological behavior by sub-watershed. The discretization of land use has retained the seven classes of land use (Fig. 9).

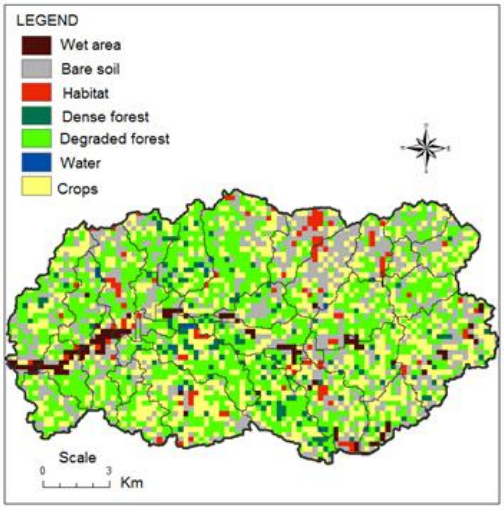

Fig. 9. Land cover map by sub watershed

However, for pedology, only one soil class was obtained in the watershed: this is the ferric Acrisols type with Af24-2a-1028 code corresponding to Ferric Acrisol (Fig. 10) in the FAO soil data base.

3.1.5 Hydrological Response Units (HRU) and watershed configuration

For this study, 213 HRUs were obtained and are divided into 39 sub watersheds. Each HRUs has its specificity in terms of hydrological behavior. This large number of HRUs reflects the distributed nature of the SWAT model (Fig. 11). Thus, it possible to simulate the watershed hydrology by taking into account the spatio-temporal variation of the watershed surface state. As the watershed is a complex system, its discretization (distribution) into HRU is an asset for hydrological modeling and minimizes simulation errors and approaches reality as much as possible. The watershed configuration provided the necessary databases. Since the SWAT model has more than a hundred parameters, only the database of land use and soil types is presented in the results (Figs. 12 and 13). This database provided by the SWAT model is very flexible although colossal and requiring a lot of calculation and analysis. Updating the data becomes easy once the configuration is complete. Although in perpetual change, the parameters of the hydrological catchment can always be updated under the SWAT model in order to adapt it to the realities of the moment.

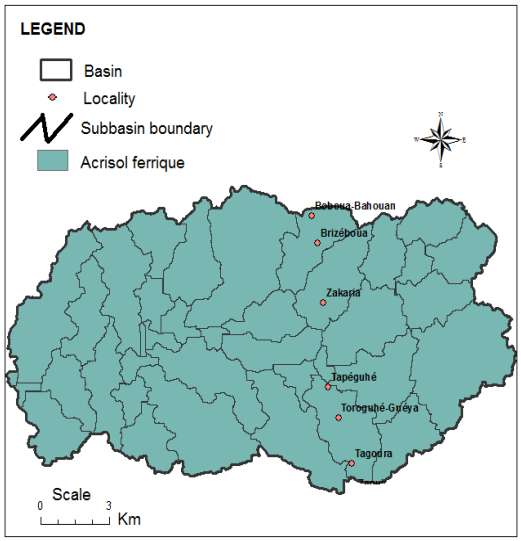

Fig. 10. Soil map by sub watershed

3.2 Discussion

Watershed delineation and hydrographic network extraction resulted in 39 sub-watersheds and a Gravelius (KG) compactness index of 1.98, indicating an elongated watershed. Its elongated shape will induce low peak flow rates. On the other hand, the low peak flows will cause a large deposition of sediments at the outlet where the Lobo water reservoir is located. These results are consistent with those derived from the work of Maiga et al. [24]. Indeed, the work done by these authors on the Lobo River reservoir in the city of Daloa in Côte d'Ivoire reveals a state of hyper-eutrophy after only a quarter century of the

dam life. The transparency measured on reading the Secchi disk is 0.8 m and the dissolved oxygen of 2 mg/l measured in surface drops to 0 from 1 m depth. The measured soluble COD is 100 mg/l. The degraded forest occupies 37% of the watershed followed by agricultural land occupying 30% of the territory. The forest heritage has gradually deteriorated in recent years [17,25]). In the basin, the degraded forest has become more and more the dominant element of this vegetation marked by the farm with a landscape where alternating crops and fallows. These percentages show that the watershed is very solicited for agriculture and is progressively deforested. This predisposes the area to the phenomenon of water erosion of soils. A sediment transport to the outlet where the Lobo water reservoir is located would occur. This situation could explain the problem of eutrophication currently observed on the water of Lobo. The maximum temperature obtained with the SWAT model over the period 1979-2017 is between 27 and 37ºC. The maximum value of maximum temperature obtained in this study is higher than that obtained by Goé B. [26] which is 31.3ºC over the period 1951-2005. This difference could come from the input data. The minimum temperature is between 18 and 23ºC. This range of minimum temperature values contains that obtained by Goé B. [26] which is 21.64ºC. However, the SWAT model overestimates this value. This difference would be related to sources and periods of data. The average monthly rainfall estimated by the SWAT model varies from 17 to 262 mm of rainfall over the entire watershed. Comparing the maximum value (262 mm) with that observed at the Daloa station, which is very close to the Lobo reservoir, which is 180 mm according to Goé B. [26], one still notice an overestimate by the SWAT model.

The DEM used in this study has a spatial resolution of 30 m. A DEM resolution of 10 m would be desirable in order to perfect the results of the modeling. There is also a problem of homogeneity or uniformity of the whole image: some areas are better treated if they have been rotated at one angle, but others are not. To solve this problem of error, some authors [27] advocate the addition of a random error. In a study of the effect of vertical errors in a DEM on the determination of runoff directions [28], it is noted that this problem is not to be neglected, especially for flat areas. The author concludes that further analyzes would be needed and a method to quantify the impacts on hydrological models would need to be developed. In order to simulate the introduction of an error in a DEM, a random error, the type of which is suggested by the acquisition method, can be added to it.

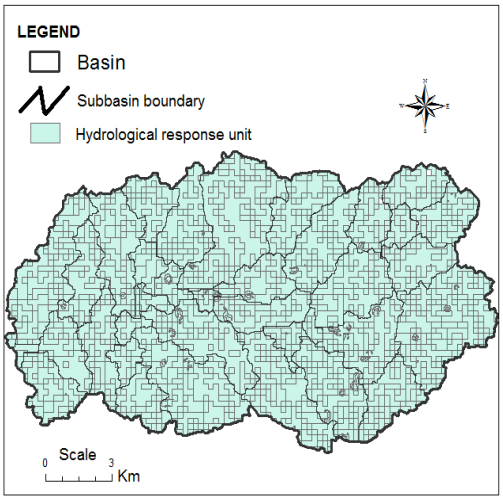

Fig. 11. HRU distribution by sub basin

With regard to the land cover and the soil maps, the major problem remains the scale. The FAO soil map has a scale of 1/5000 000 and dates back to 1981. The land cover map is derived from the sentinel-2 image of 22 February 2018. These rough scales generate losses of information on maps and create uncertainties in the model. In addition, the combination of these data from different dates biases the results of the simulation. Many data sources exist to document the evolution of land use such as aerial photographs and satellite images at higher or lower resolution [29]. These data differ in resolution and date of shooting. Geographers generally use several shots to map land use in a given year. In the Yzeron basin, in 2008, Jacqueminet et al. [29] find a casting percentage equal to 2.2% when calculated from a photo-air (resolution 0.50 m) and 17% when calculated from a satellite image SPOT (resolution 2.44 m). To reduce these effects, the different sources of data [29] or the data of the same year [30] can be combined to construct a synthetic Land cover map. Several authors have shown that the resolution of input data has an impact on simulation results [31,32]. The choice of one data type can also greatly influence the hydrological modeling results as the simulated surface runoff is generally related to the percentage of impervious zones, which is obtained by interpreting the land cover data. Branger et al. [33] showed that this choice has all the more visible impacts on the modeling that the variables

of interest are the components of the flow (runoff, subsurface flow, base flow) and that the evaluation relates to the seasonal dynamics. The interest of HRUs in understanding hydrological processes is twofold [34]. First, these units make it possible to simplify the representation of the physiographic characteristics of the basin and to take into account their spatial variability. Secondly, the URHs are supposed to generate different hydrological responses in the watershed. The functioning of the watershed is thus assimilated to that of a set of interconnected reservoirs. It is each unit and not the entire basin that is represented by a set of interconnected reservoirs, which gives results closer to reality [35]. The division of space in HRU has been adopted in the works of Indarto [36] and Kouamé et al. [10] respectively in the catchment areas of N'zô in Ivory Coast and Orb in France to model surface runoff.

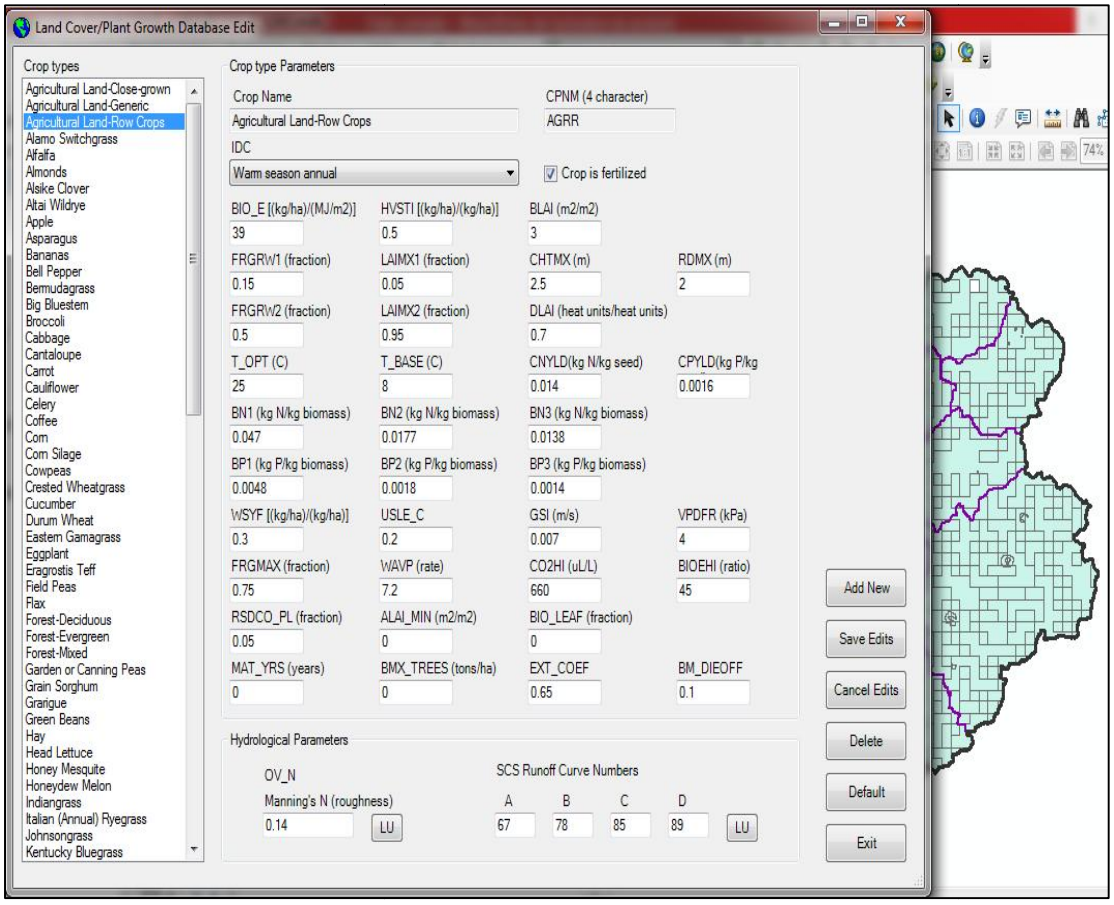

Fig. 12. Example of a land cover database

Table 1. Confusion matrix from the supervised classification of land cover types

Land use class	Dense forest	Degraded forest	Habitat	Grassy vegetation	Agriculture	Water	Wet area
Dense forest	84.2	0.19	0	0	27.4	0	0
Degraded forest	12.29	54.55	0	1.46	0.2	0	0.18
Habitat	0	0	95.58	0.29	0.05	0	0
Grassy vegetation	0	2.15	2.81	72.25	0.5	0	2.15
Agriculture	3.51	43.12	1.61	26	71.85	0	5.32
Water	0	0	0	0	0	100	0
Wet area	0	0	0	0	0	0	92.35
Total	100	100	100	100	100	100	100

Table 2. SWAT model hydro statistical parameters

Station	WLATITUDE	WLONGITUDE	WELEV	RAIN_YRS	TMPMX1	TMPMX2	TMPMX3	TMPMX4	TMPMX5
w67-66	6.71	-6.56	307	35	35.25	36.05	35.54	34.38	32.29
w70-66	7.03	-6.56	286	35	35.51	36.49	36.19	35.02	32.97
w67-63	6.71	-6.25	265	35	35.38	36.27	35.81	34.68	32.44
w70-63	7.03	-6.25	302	35	35.68	36.77	36.54	35.41	33.26

Table 3. SWAT model hydro statistical parameters (continued)

TMPMX6	TMPMX7	TMPMX8	TMPMX9	TMPMX10	TMPMX11	TMPMX12	TMPMN1	TMPMN2	TMPMN3
29.76	27.71	27.30	28.78	30.83	32.10	33.21	19.53	21.42	22.43
30.41	28.15	27.62	29.16	31.15	32.27	33.58	18.95	21.26	22.55
29.88	27.85	27.39	28.90	30.95	32.20	33.28	19.70	21.54	22.45
30.61	28.33	27.80	29.32	31.27	32.42	33.68	19.34	21.51	22.67

Table 4. SWAT model hydro statistical parameters (continued)

TMPMN4	TMPMN5	TMPMN6	TMPMN7	TMPMN8	TMPMN9	TMPMN10	TMPMN11	TMPMN12	TMPSTDMX1
22.60	22.17	21.29	20.43	20.53	21.09	21.43	21.26	20.24	1.99
22.69	22.17	21.29	20.44	20.52	21.01	21.28	21.02	19.71	1.87
22.59	22.14	21.27	20.41	20.52	21.08	21.40	21.27	20.35	2.02
22.76	22.18	21.30	20.47	20.56	21.07	21.35	21.16	19.97	1.91

Table 5. SWAT model hydro statistical parameters (continued)

TMPSTDMX2	TMPSTDMX3	TMPSTDMX4	TMPSTDMX5	TMPSTDMX6	TMPSTDMX7	TMPSTDMX8	TMPSTDMX9	TMPSTDMX10	TMPSTDMX11
2.61	3.22	3.05	3.06	2.80	2.54	2.55	2.91	2.58	1.94
2.45	3.14	3.13	3.17	2.90	2.62	2.65	2.98	2.57	1.97
2.62	3.29	3.11	3.10	2.81	2.58	2.58	2.92	2.60	1.99
2.49	3.18	3.23	3.22	2.93	2.70	2.70	2.99	2.60	1.99

Table 6. SWAT model hydro statistical parameters (continued)

TMPSTDMX12	TMPSTDMN1	TMPSTDMN2	TMPSTDMN3	TMPSTDMN4	TMPSTDMN5	TMPSTDMN6	TMPSTDMN7	TMPSTDMN8	TMPSTDMN9
2.18	3.27	1.96	0.99	0.75	0.75	0.80	0.84	0.82	0.71
2.17	3.74	2.53	1.04	0.80	0.77	0.82	0.85	0.85	0.79
2.21	3.16	1.89	0.99	0.77	0.75	0.79	0.84	0.82	0.71
2.21	3.50	2.37	1.06	0.80	0.77	0.79	0.84	0.83	0.75

Table 7. SWAT model hydro statistical parameters (continued)

TMPSTDMN10	TMPSTDMN11	TMPSTDMN12	PCPMM1	PCPMM2	PCPMM3	PCPMM4	PCPMM5	PCPMM6	PCPMM7
0.81	1.08	2.29	24.55	52.38	119.20	176.40	208.18	161.24	149.64
0.95	1.24	2.76	17.23	41.25	107.83	170.62	199.16	156.90	145.77
0.79	1.03	2.18	26.09	51.99	119.48	178.46	210.44	156.21	135.99
0.88	1.12	2.55	20.38	43.12	111.04	173.33	198.12	150.62	130.60

Table 8. SWAT model hydro statistical parameters (continued)

PCPMM8	PCPMM9	PCPMM10	PCPMM11	PCPMM12	PCPSTD1	PCPSTD2	PCPSTD3	PCPSTD4	PCPSTD5
177.29	260.51	204.24	71.13	26.94	2.38	5.16	8.49	11.66	10.10
183.85	262.33	186.84	59.45	21.90	1.89	4.43	9.50	11.54	11.14
163.52	246.34	193.97	68.93	27.62	2.94	4.99	8.14	12.52	10.09
164.45	246.13	182.55	63.65	23.50	2.72	4.35	8.72	11.71	11.34

Table 9. SWAT model hydro statistical parameters (continued)

PCPSTD6	PCPSTD7	PCPSTD8	PCPSTD9	PCPSTD10	PCPSTD11	PCPSTD12	PCPSKW1	PCPSKW2	PCPSKW3
7.11	7.40	7.08	10.19	9.50	2.78	1.86	7.90	7.95	8.30
8.39	7.61	8.63	10.92	8.60	2.76	2.74	7.49	6.77	10.52
6.96	7.11	6.98	10.17	8.56	2.70	1.89	10.15	8.66	5.91
7.86	7.07	8.12	11.19	7.82	2.92	2.79	12.46	7.25	6.38

Table 10. SWAT model hydro statistical parameters (continued)

PCPSKW4	PCPSKW5	PCPSKW6	PCPSKW7	PCPSKW8	PCPSKW9	PCPSKW10	PCPSKW11	PCPSKW12	PR_W1_1
6.08	5.09	5.42	6.00	4.27	4.31	5.47	2.14	5.34	0.19
5.44	4.81	7.24	5.42	5.97	5.38	6.18	2.69	20.17	0.18
6.09	4.18	5.26	7.63	5.12	5.08	5.28	2.44	4.93	0.19
5.10	4.87	6.05	6.30	6.44	6.82	4.58	2.71	18.57	0.18

Table 11. SWAT model hydro statistical parameters (continued)

PR_W1_2	PR_W1_3	PR_W1_4	PR_W1_5	PR_W1_6	PR_W1_7	PR_W1_8	PR_W1_9	PR_W1_10	PR_W1_11
0.36	0.46	0.78	0.88	0.80	1.00	0.00	0.00	1.00	0.71
0.32	0.49	0.64	0.85	0.89	1.00	0.00	0.00	1.00	0.64
0.36	0.49	0.65	0.94	0.71	1.00	1.00	0.00	1.00	0.58
0.32	0.46	0.63	0.84	0.80	1.00	1.00	0.00	1.00	0.64

Table 12. SWAT model hydro statistical parameters (continued)

PR_W1_12	PR_W2_1	PR_W2_2	PR_W2_3	PR_W2_4	PR_W2_5	PR_W2_6	PR_W2_7	PR_W2_8	PR_W2_9
0.33	0.84	0.85	0.93	0.96	0.99	1.00	1.00	1.00	1.00
0.31	0.79	0.81	0.90	0.94	0.97	0.99	1.00	1.00	1.00
0.34	0.84	0.84	0.92	0.96	0.98	1.00	1.00	1.00	1.00
0.33	0.78	0.80	0.90	0.95	0.98	0.99	0.99	1.00	1.00

Table 13. SWAT model hydro statistical parameters (continued)

PR_W2_10	PR_W2_11	PR_W2_12	PCPD1	PCPD2	PCPD3	PCPD4	PCPD5	PCPD6	PCPD7
1.00	0.98	0.88	16.69	19.86	26.67	28.39	30.53	29.83	30.86
1.00	0.96	0.81	14.28	17.72	25.75	27.53	30.06	29.72	30.86
1.00	0.98	0.88	16.56	19.61	26.56	28.17	30.47	29.78	30.92
1.00	0.96	0.81	14.00	17.36	25.56	27.67	30.11	29.69	30.78

Table 14. SWAT model hydro statistical parameters (continued)

PCPD8	PCPD9	PCPD10	PCPD11	PCPD12	RAINHHMX1	RAINHHMX2	RAINHHMX3	RAINHHMX4	RAINHHMX5
31.00	30.00	30.97	29.11	22.37	2.64	5.80	9.57	14.21	13.75
31.00	30.00	30.91	28.34	18.97	2.07	4.90	10.43	14.09	15.22
30.91	30.00	30.97	29.11	22.66	3.02	4.93	9.52	14.83	13.68
30.94	30.00	30.94	28.26	19.40	2.67	4.81	10.00	13.78	14.95

Table 15. SWAT model hydro statistical parameters (continued)

RAINHHMX6	RAINHHMX7	RAINHHMX8	RAINHHMX9	RAINHHMX10	RAINHHMX11	RAINHHMX12	SOLARAV1	SOLARAV2	SOLARAV3
9.13	9.83	9.12	12.68	11.29	3.39	2.20	20.14	20.14	20.05
10.83	10.43	10.35	13.82	10.99	3.26	2.33	20.36	20.47	20.27
8.85	8.79	8.92	12.92	10.47	3.33	2.25	20.07	20.09	20.03
10.33	9.50	9.97	14.06	10.05	3.63	2.42	20.29	20.33	20.13

Table 16. SWAT model hydro statistical parameters (continued)

SOLARAV4	SOLARAV5	SOLARAV6	SOLARAV7	SOLARAV8	SOLARAV9	SOLARAV10	SOLARAV11	SOLARAV12	HMDT1
19.76	19.03	16.85	14.04	13.29	16.24	18.42	17.93	18.59	0.59
19.87	19.39	17.66	14.85	13.95	16.95	18.74	18.22	18.92	0.55
19.81	19.17	17.09	14.35	13.52	16.41	18.48	18.00	18.52	0.59
19.77	19.37	17.78	14.97	14.03	16.91	18.65	18.11	18.78	0.54

Table 17. SWAT model hydro statistical parameters (continued)

HMD2	HMD3	HMD4	HMD5	HMD6	HMD7	HMD8	HMD9	HMD10	HMD11
0.65	0.71	0.76	0.83	0.86	0.87	0.89	0.89	0.87	0.83
0.60	0.68	0.74	0.80	0.84	0.85	0.88	0.89	0.86	0.81
0.64	0.70	0.75	0.82	0.86	0.86	0.88	0.89	0.87	0.83
0.60	0.67	0.73	0.79	0.84	0.85	0.87	0.88	0.86	0.81

Table 18. SWAT model hydro statistical parameters (continued)

HMD12	WNDAV1	WNDAV2	WNDAV3	WNDAV4	WNDAV5	WNDAV6	WNDAV7	WNDAV8	WNDAV9	WNDAV10	WNDAV11	WNDAV12
0.71	1.42	1.61	1.71	1.68	1.57	1.59	1.63	1.60	1.41	1.29	1.23	1.27
0.67	1.43	1.64	1.77	1.77	1.66	1.68	1.73	1.67	1.44	1.31	1.29	1.31
0.71	1.46	1.65	1.75	1.74	1.62	1.64	1.69	1.65	1.45	1.33	1.27	1.31
0.67	1.48	1.68	1.82	1.82	1.72	1.73	1.78	1.72	1.47	1.35	1.33	1.36

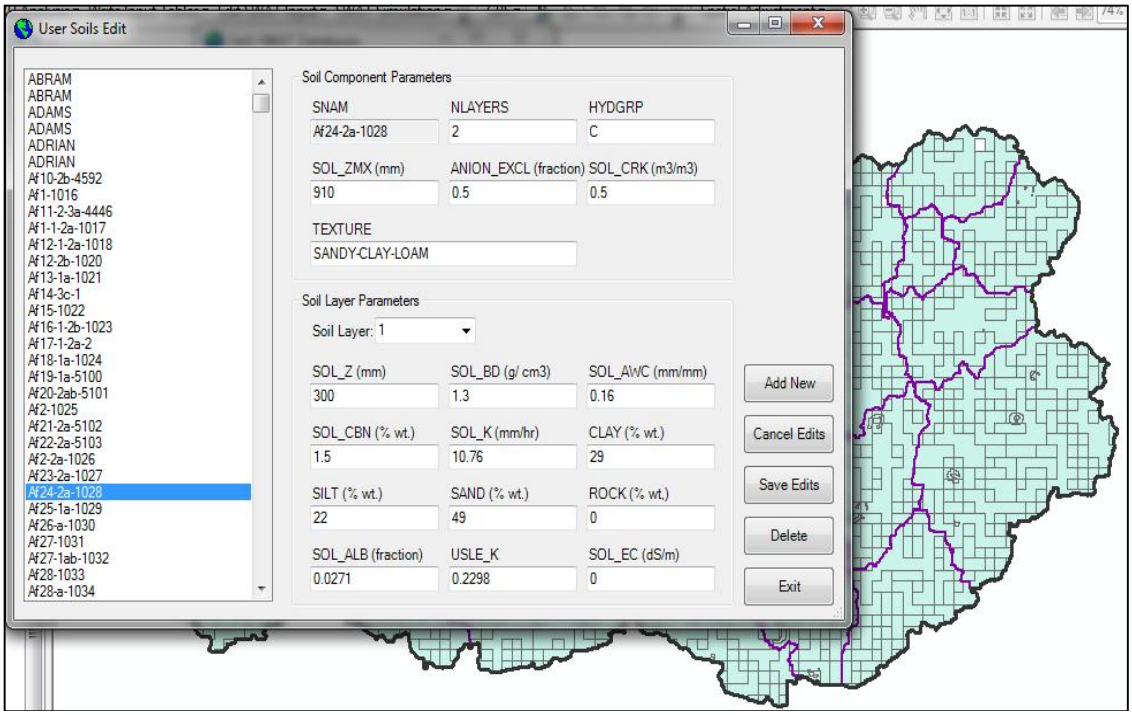

Fig. 13. Example of soil database

4. CONCLUSION

This study has shown that because of the elongated form of the Lobo watershed, it is exposed to the phenomenon of eutrophication. This phenomenon is accelerated by agricultural activities upstream of the Lobo reservoir. The study indicated that agriculture occupies 30% of the territory; which resulted in forest degradation of 37%. Estimation of the hydro statistic parameters revealed that the mean daily maximum and minimum temperatures in the month range from 27 to 37ºC and from 18 to 23ºC, respectively. As for the average daily rainfall in the month, it varies from 17 to 262 mm. Compared with the temperatures, it is retained that the rainfall varies with a standard deviation ranging from 1.8 to 12.52 mm against 0.7 to 3.5ºC standard deviation of the temperatures. The watershed configuration has discretized it into 213 HRUs and 39 sub-basins. This large number of HRUs shows the distributed nature of the SWAT model which is therefore adapted to our agricultural catchment areas.

ACKNOWLEDGEMENT

The authors wish to thank Professor Stoleriu Cristian from Alexandru Ioan Cuza at Faculty of Geography in Romania for his beneficial suggestions. This work was supported in part by grants from ‘’Agence Universitaire de la Francophonie’’ (Eugen Ionescu Program).

COMPETING INTERESTS

Authors have declared that no competing interests exist.

REFERENCES

1. Rissons M, Bocquillon C. Un modèle hydrologique spatialisé SIG, base de données et mécanismes hydrologiques : Application of Geographic Information Systems in Hydrology and Water Resources Management. Proceedings of the Vienna Conference. 1996; IAHS Publ. no. 235. French
2. Villeneuve JP, Hubert P, Mailhot A, Rousseau AN. La modélisation hydrologique et la gestion de l'eau. Revue des sciences de l'eau. 1998;11:19-39. French
3. Bewket W, Sterk G. Dynamics in land cover and its effect on stream flow in Chemoga watershed, blue Nile basin, Ethiopia. Hydrological Process. 2005;19: 445-458.

4. Dupont J, Smitz J, Rousseau AN, Mailhot A, Gangbazo G. Utilisation des outils numériques d'aide à la décision pour la gestion de l'eau. Revue des sciences de l'eau. numéro spécial: 1998;5-18. French
5. Kouamé K, Kouamé A, Kouassi KFA, Oularé S, Adon C-RG, Bernier M. Mise en place d'une base de données pour une modélisation hydrologique distribuée du bassin versant du Bandama (Côte d'Ivoire) : apport d'un modèle numérique d'altitude, de la télédétection et du SIG Physitel. Afrique Science. 2011;7(2):94-114. French
6. Chocat B. Techniques alternatives, Assainissement, Bassin de retenue. Encyclopédie de l'hydrologie Urbaine et de l'assainissement. Ed.Tec et Doc, Lavoisier; 1997. French
7. Refsgaard JC. Parameterization, calibration, and validation of distributed hydrological models. Journal of Hydrology. 1997;198(1-4):69-97.
8. Refsgaard JC, Storm B. Construction, calibration, and validation of hydrological models. In: Abbot MB, Refsgaard JC, editors . Distributed Hydrologic Modeling. Dordrecht, The Netherlands: Kluwer Academic Publishers; 1996.
9. Wischmeier WH, Smith DD. Predicting Rainfall Erosion Losses. Agriculture Handbook 537, United States Department of Agriculture, Science and Education Administration; 1978.
10. Kouamé KF, Bernier M, Fortin JP, Lefebre R, Biemi, J. Application du modèle hydrologique distribué 'HYDROTEL' à la simulation des écoulements des eaux en milieu tropical humide : cas du bassin versant du N'zo en Côte d'Ivoire. 12è congrès de l'AQT, Chicoutimi; 2005. French
11. Wagena MB, Collick AS, Ross AC, Najjar RG, Rau B, Sommerlot AR, et al. Impact of climate change and climate anomalies on hydrologic and biogeochemical processes in an agricultural catchment of the Chesapeake Bay watershed, USA. Science of Total Environment. 2018;1443-1454.
12. Bai J, Shen Z, Yan T. Effectiveness of vegetative filter strips in abating fecal coliform based on modified soil and water assessment tool. International Journal of Environmental Science and Technology. 2016;13:1723-1730.
13. Koua TJ, Jourda JP, Kouamé KJ, Anoh KA, N'dri WK, Lazar G, et al. Effectivness of soil and water assessment tool model to simulate water flow in a large agricultural complex watershed: case of Buyo lake basin, West of Côte d'Ivoire. Environmental Engineering and Management Journal. 2014;13:735-1742. Available:https://doi.org/10.30638/eemj.2014.193
14. Koua TJ, Jourda JP, Kouame KJ, Anoh KA, Balin D, Lane S. Potential climate change impacts on water resources in the Buyo Lake Basin (Southwest of Ivory Coast). International Journal of Innovation and Applied Studies. 2014;8:1094-1111.
15. Anoh K, Koua T, Eblin S, Kouamé K, Jourda J. Modelling Freshwater Availability Using SWAT Model at a Catchment-Scale in Ivory Coast. Journal of Geoscience and Environment Protection. 2017;5:70-83. DOI:10.4236/gep.2017.513005
16. Avenard JM. Aspect de la géomorphologie. In : Mémoire ORSTOM. Milieu naturel de la Cote d'Ivoire. Paris, France; 1971. French
17. Brou Y. Climat, mutations socio-économiques et paysages en Côte d'Ivoire. Mémoire de synthèse présentés en vue de l'obtention de l'Habilitation à Diriger des Recherches. Université des Sciences et Technologies de Lille. 2005; 106. French
18. Nachtergaele F, Velthuizen HV, Verest L. Harmonized world soil database version1.1. 2009; [Accessed on october, 2012] Available:http://www.fao.org/fileadmin/templates/nr/documents/HWSD/HWSD_Documentation.pdf.
19. Jenson SK, Domingue JO. Extracting topographic structures from digital elevation data for geographic information system analysis. Photogrammetric engineering and remote sensing. 1998; 54(11):1593–1600.
20. Charleux-Demargne J. Qualité des Modèles Numériques de Terrain pour l'hydrologie. Application à la caractérisation du régime de crue des bassins versants. Thèse ENSG. Université de Marne la Vallée. 2004;350. French
21. FAO. The state of food and agriculture. Report. 1998;389.
22. Puech C. Détermination des états de surface par télédétection pour caractériser les écoulements des petits bassins versants. Application à des bassins en zone méditerranéenne et en zone tropicale

sèche. Thèse de Doctorat, Université Joseph Fourier. 1993;230. French
23. Arnold JG, Kiniry JR, Srinivasan, Williams RJR, Haney EB, Neitsch SL. Soil and Water Assessment Tool, Input/ Output File documentation version 2009; 2011. Available:http://swat.tamu.edu/media/19754/swat-io-2009.pdf.
24. Maïga A, Denyigba K. Eutrophication of small dams in West Africa. The case of Lobo dam (Côte d'Ivoire) in: 4th interregional conference on Environment and water. Fortalega (Brasil). 2001;27-31.
25. N'go AY, Kouadio AZ, Déguy JPA, Hien AS, Goula ABT, Savané I. Influence de la dynamique de l'occupation du sol sur la quantité de perte de sol au Sud du bassin versant du Sassandra (Côte d'Ivoire), International Journal of Advanced Research. 2018;6(4):830-838.
26. Goé B. Evaluation de l'impact des changements climatiques sur les ressources en eau du bassin versant de la Lobo à Nibéhibé: Centre-Ouest de la Côte d'Ivoire. Mémoire de Master en Génie de l'Eau et Environnement, Université Jean Lorougnon Guédé, Côte d'Ivoire. 2019;50. French
27. Quentin E. Optimisation des paramètres de la procédure géomatique d'extraction des caractéristiques hydrologiques d'un bassin versant à partir d'un modèle numérique d'altitude. Thèse de doctorat. Université de Sherbrooke. 1999;127. French
28. Veregin H. The Effects of Vertical Error in Digital Elevation Models on the determination of flow-path Direction. Cartography and Geographic Information Systems. 1997;24(2):67-79.
29. Jacqueminet C, Kermadi S, Michel K, Béal D, Branger F, Jankowsky S, Braud I. Land cover mapping using aerial and VHR satellite images for distributed hydrological modelling of periurban catchments: Application to the yzeron catchment (lyon, france). Journal of Hydrology. 2013;485: 68-83.
30. Villarreal M L, Norman LM, Wallace CSA., Van Riper C. A multitemporal (1979-2009) land use/land-cover dataset of the binational santa cruz watershed. US Geological Survey, Reston, Virginia. Technical report. 2011;113.
31. Cotter AS, Chaubey I, Costello TA, Soerens TS, Nelson MA. Water quality model output uncertainty as affected by spatial resolution of input data. Journal of the American Water Resources Association. 2003;39(4):977-986.
32. Bormann N, Breuer, Groff L, Huisman TJ, Croke B. Assessing the impact of land use change on hydrology by ensemble modelling: Model sensitivity to data aggregation and spatial (re-) distribution. Advances in Water Resources. 2009;32(2): 171-192.
33. Branger F, Kermadi S, Jacqueminet C, Michel K, Labbas M, Krause P, Kralisch S, Braud I. Assessment of the influence of land use data on the water balance components of a peri-urban catchment using a distributed modelling approach. Journal of Hydrology. 2013;505:312-325.
34. Fortin JP, Turcotte R, Massicotte S, Moussa R, Fitzback J, Villeneuve JP. A distributed watershed model compatible with remote sensing and GIS data: Application to Chaudière watershed. Journal of Hydrologic Engineering. 2001; 6(2):100-108.
35. Ambroise B. La dynamique du cycle de l'eau dans un bassin versant : processus, facteurs, modèles. Ecole Polytechnique Fédérale de Lausanne, HGA Bucarest. 1999;206. French
36. Indarto K. Découpages spatiaux et conséquences sur le bilan hydrologique. Thèse de Doctorat, Université de Montpellier. 2002;258. French

Peer-review history:
The peer review history for this paper can be accessed here:
http://www.sdiarticle4.com/review-history/53078